SIMULATION OF SEMICONDUCTOR DEVICES AND PROCESSES Vol. 3
Edited by G. Baccarani, M. Rudan - Bologna (Italy) September 26-28, 1988 - Tecnoprint

Physical Modelling of GaAs Photodetectors

D. M. Barry, S. P. Platt,
C. M. Snowden, M. J. Howes and R. E. Miles

Microwave Solid State Group,
Department of Electrical and Electronic Engineering,
The University of Leeds, Leeds LS2 9JT, United Kingdom.

Introduction

Modern solid state optoelectronic systems are now capable of operating at such high frequencies that it has become necessary to employ microwave and even millimetric wave technology in their applications. Sobol (1987) summarises the present achievements made in optical communications which range from the commercially available systems with transmission rates of 500 Mbit/s at 1.3 μm wavelengths to laboratory tests where 4 Gbit/s have been reported at 1.55 μm wavelengths. The most common type of devices used for high speed optical detection are p-i-n and Schottky barrier photodiodes. Some applications have also employed optically controlled MESFETs.

This paper concentrates on the theoretical understanding and modelling of GaAs Schottky photodiodes. Although the basic principles of optical detection are well understood, the device response to ultrashort pulses of the order of picoseconds can only be theoretically determined by numerical simulation. Two separate methods are considered, a bipolar drift-diffusion model and a Monte Carlo model. Results from these simulations are presented, along with theoretically determined hole transport characteristics for GaAs, obtained using the Monte Carlo technique.

The Device

The type of photodetectors primarily under investigation are high speed photodiodes described by Parker et. al. (1985, 1986, 1987) which are fabricated with an Indium Tin Oxide (ITO) Schottky contact to n-type Gallium Arsenide (GaAs). This type of device has been reported to have a bandwidth of 110 GHz. The basic structure of device is shown in *fig. 1*. Optical illumination at wavelengths $\leq 880\,nm$ is through the ITO which is transparent at these frequencies. Due to the simple linear structure and large aspect ratio it is quite reasonable to use a one dimensional model of the device as shown in *fig. 2(a)*.

The energy-band diagram for the reverse biased-device is shown in *fig.2(b)*. Optical generation occurs in both the n^- and n^+ regions, where the generated carriers come under the influence of high and low electric fields respectively. In the n^- region, therefore, they attain velocities close to

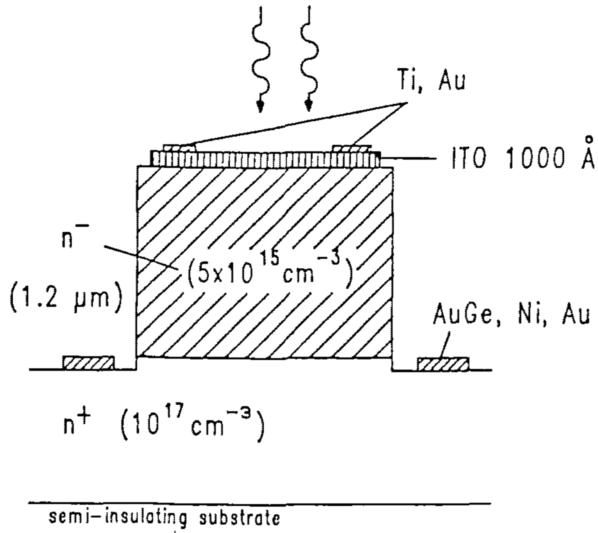

Fig. 1 ITO/GaAs Schottky photodiode

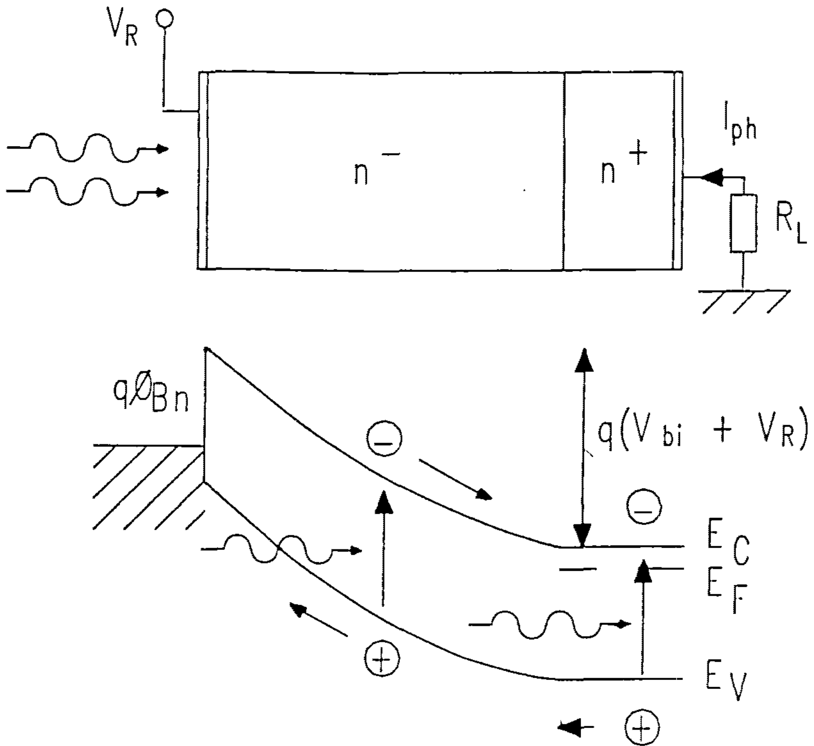

Fig. 2 (a) Schottky photodiode (b) Energy band diagram

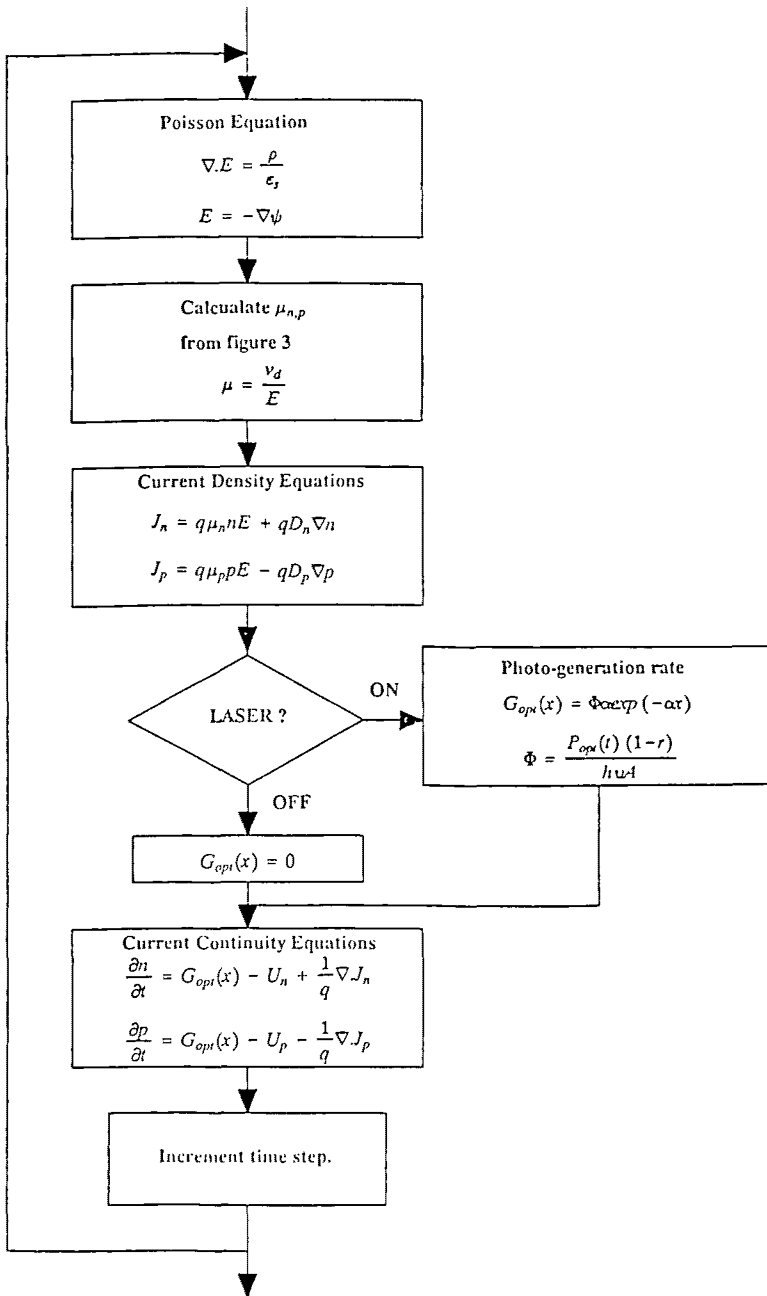

Fig. 3 System of equations used in bipolar drift-diffusion model

saturation, whereas slow diffusion processes dominate transport in the n^+ region.

The Drift-Diffusion Model

The device has been simulated using a bipolar drift-diffusion model of the type described by Snowden (1986). A similar approach was used by Peterson (1987) to model Si interdigitated photoconductors, which successfully predicted the device response. Here the work has been extended to include a Schottky barrier model and the field dependent carrier transport properties of GaAs. A number of improvements have also been made to the original work of Barry et. al. (1988).

The discretisation of the drift-diffusion model enables the set of equations in *fig. 3* to be solved by numerical techniques subject to the boundary conditions described below. For the finite-difference Poisson solver, these consist of fixed potentials representing the barrier height of $\approx$ 0.9 V at the Schottky contact and the DC bias applied to the ohmic contact.

The electron mobility is calculated a function of electric field, doping and temperature by the empirical expression given by Snowden (1983). An expression for the hole mobility as a function of the electric field strength (E) has been derived from the hole transport properties calculated by the Monte Carlo model shown in *fig. 4*.

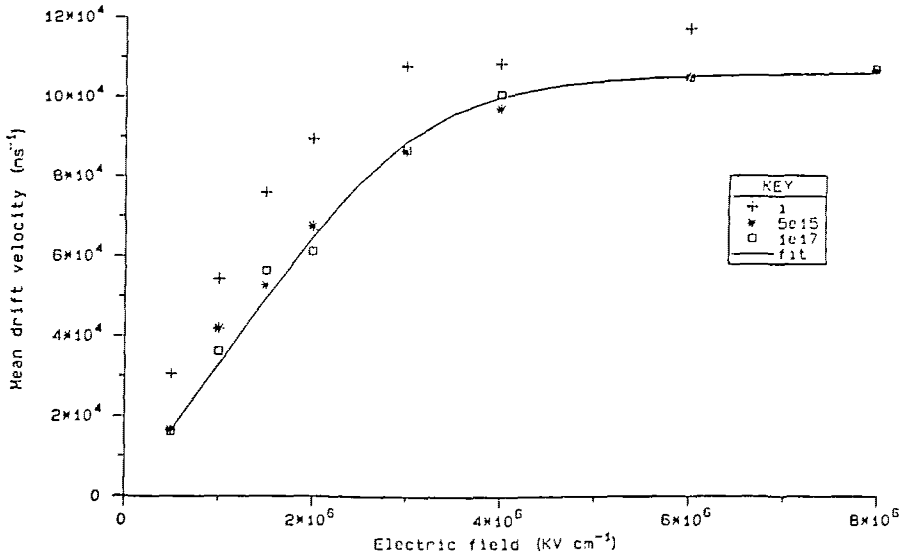

Fig. 4 Velocity field curves for holes in GaAs at 300K

$$\mu_p(\mathrm{E}) = \frac{\mu_{low}}{\left(1 + \left(\frac{\mu_{low}\mathrm{E}}{v_{sat}}\right)^{\beta}\right)^{\frac{1}{\beta}}} \quad (cm^2V^{-1}s^{-1}) \qquad (1)$$

where the low field mobility $\mu_{low} = 330\, cm^2V^{-1}s^{-1}$, the hole saturated velocity $v_{sat} = 1.06\times10^7\, cms^{-1}$ and $\beta = 5$.

In order to avoid numerical instability when solving the current continuity equations it is necessary to re-write them in terms of Bernoulli functions as described by Scharfetter and Gummel (1969). The boundary conditions are set by fixing the electron and hole concentrations for the the first and last element in the arrays. At the Schottky contact the electron concentration is calculated from the effective density of states in the conduction band (N_c) and the Schottky barrier height (Φ_{Bn}) and is given by

(2) $$n = N_c \exp\left(\frac{-q\Phi_{Bn}}{k_B T}\right) \qquad (cm^{-3})$$

where q is the electronic charge (C), k_B the Boltzmann constant (JK^{-1}) and T the device temperature (K). The n^+ doping concentration is held at the ohmic contact. The initial hole concentration is then calculated to be:

(3) $$p = \frac{n_i^2}{n} \qquad (cm^{-3})$$

where n_i is the intrinsic carrier concentration.

The thermal generation-recombination rate is modelled using the Schockly-Hall-Read model where the net rate is given as:

(4) $$G_{thermal} = \frac{n_i^2 - pn}{\tau_n(p + p_t) + \tau_p(n + n_t)} \qquad (cm^{-3}s^{-1})$$

where τ_n and τ_p are the carrier lifetimes. For trap centres in the middle of the band gap $n_t = p_t = n_i$.

The optical generation rate is a function of the exponential absorption which occurs when an optical electromagnetic wave passes through the device and is given by:

(5) $$G_{opt}(x) = \Phi\alpha exp(-\alpha x) \qquad (cm^{-3}s^{-1})$$

where x is the distance into the device (cm) and α the absorption coefficient (cm^{-1}). The light flux density Φ, may be written in terms of incident optical power P_{opt} (W), the photon energy $h\nu$ (J), the photosensitive device area A (cm^2) and the reflection coefficient r:

(6) $$\Phi = \frac{P_{opt}(t)\,(1-r)}{h\nu A} \qquad (s^{-1}cm^{-2})$$

Making $P_{opt}(t)$ a function of time allows the laser to be switched on and off at different time steps during the simulation and has the added advantage of allowing the optical pulse to be shaped.

The simulation is capable of calculating both time dependent and steady-state results. For the time dependent solution successive under relaxation is used to ensure the current continuity equations will converge successfully. A solution for the steady-state case can be found much more quickly by recognising that

(7) $$\frac{\partial n}{\partial t} = 0 \quad \text{and} \quad \frac{\partial p}{\partial t} = 0$$

The continuity equations for the whole device may then be written as

$$\left[\mathbf{A}_{n,p}\right]\left[\mathbf{c}_{n,p}\right] = \left[\mathbf{R}_{n,p}\right] \tag{8}$$

where $\mathbf{A}_{n,p}$ is a square tridiagonal matrix made up of the Bernoulli functions, $\mathbf{c}_{n,p}$ are the corresponding discretised carrier concentrations and the vector $\mathbf{R}_{n,p}$ is made up of the generation rates and boundary conditions described above. This equation is solved directly using LU decomposition. In order to ensure convergence the carrier concentrations must be calculated after each iteration of the Poisson equation. For highly doped regions it is also necessary to either increase the number of discretised points or reduce the rate of over-relaxation in the Poisson solver.

The total current density is calculated at each time step as

$$J_{tot} = J_n + J_p + \varepsilon_o \varepsilon_r \frac{\partial E}{\partial t} \qquad (A\ cm^{-2}) \tag{9}$$

where J_n and J_p are the carrier current densities and the last term is the displacement current associated with the detector's capacitance.

The Monte Carlo Models

The Monte Carlo particle modelling technique (Jacoboni and Reggiani, 1983; Moglestue, 1986) has been used to simulate the transport of both electrons and holes in bulk GaAs, and is being applied to the modelling of photodiode structures. A flow diagram for the bulk programs is shown in *fig 5*.

The conduction band of GaAs is represented as three spherical, non-parabolic valleys at the Γ, L and X points in k-space (Littlejohn et.al. 1977). The model used for the valence band structure corresponds to that of Costato et.al. (1972), consisting of two spherical, parabolic bands degenerate at the Γ point, the split-off band being neglected. This model is considerably simpler than that of Brennan and Hess (1984), which includes all three bands and accounts for the full complexity of band structure. This simple model was chosen as there was no requirement to include anisotropic effects such as impact ionisation. The results for hole transport suggest that the assumption of parabolicity, in particular, may be inaccurate, and work is continuing to improve the model.

Scattering processes included in the models are those caused by ionised impurities, polar and nonpolar optical phonons (including electron intervalley scattering) and acoustic phonons (Nag, 1972). The dominant processes in determining carrier transport at low electric fields are those involving polar optical phonons, whilst at high electric fields nonpolar optical mechanisms (intervalley scattering for electrons) dominate.

The Monte Carlo Photodiode Simulation

The Monte Carlo procedures used to model bulk carrier transport have been incorporated into a one dimensional simulation of the photodiode of *fig. 1*. In contrast to the drift-diffusion approach which uses a greatly simplified model to describe carrier transport, the Monte Carlo technique provides, intrinsically, a complete model of carrier transport including non-stationary and hot-carrier effects.

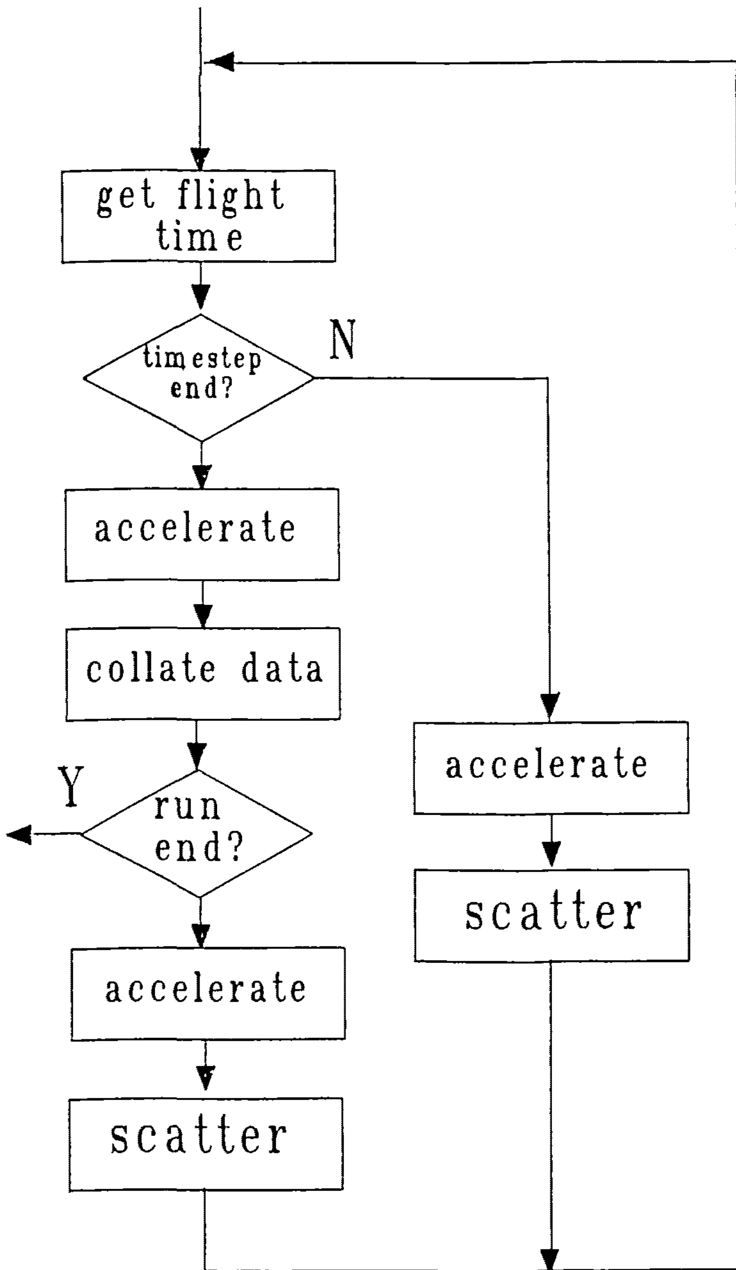

Fig. 5 Flow diagram for the Monte Carlo procedure

The Poisson equation is solved iteratively as for the drift-diffusion model. The Monte Carlo and Poisson solving procedures are carried out in succession, providing self-consistent solutions for potential, electric field and carrier concentration throughout the device.

The requirement for constant electron density at the ohmic contact is met by injecting 'cold' electrons at each time step. Particles leaving the device by either contact are lost to the simulation. Current is determined from the number of particles passing through the terminals.

Illumination of the device is accounted for at each time step. The photogeneration rate is given by:

$$N = \frac{RP_{opt}(1-r)}{q} \qquad (s^{-1}) \tag{10}$$

where N is the number of electron-hole pairs generated per second and R is the device responsivity (A/W).

The spatial distribution of optically generated electron-hole pairs (*eq. 5*) is chosen by a random number procedure thus:

$$x = \frac{\ln\left[(e^{-\alpha W}-1)r+1\right]}{-\alpha} \qquad (\text{cm}) \tag{11}$$

where x is the depth into the device at which electron-hole pairs are generated, W the device thickness (cm) and r a random number between 0 and 1. Both types of particle are initially assigned zero energy, corresponding to an input photon energy equal to the GaAs bandgap of 1.44 eV, or a wavelength of 860 nm.

Previous Monte Carlo models of optoelectronic devices have neglected electron-hole recombination (Moglestue, 1984). The effect of this process is included in this work, by means of an extra 'scattering' mechanism. The rate of recombination (*eq. 4*) is calculated at each time step for each internal node. Particles undergoing one of these events are lost to the simulation, along with their nearest neighbour of opposite charge.

Simulation Results.

Results from the bulk hole transport simulation, in the form of velocity-field curves, are shown in *fig. 4*. Comparison of these with experimental (Holway et. al., 1979) and theoretical (Brennan and Hess, 1984) results for GaAs hole mobility show good general agreement, although saturated velocities as calculated here are larger. This is in accordance with the the simplified valence band structure assumed here.

The following results have been calculated for the device of *fig. 1*. Steady-state solutions for the device with a reverse bias of 5 volts under dark and constant illuminated conditions are shown in *fig. 6*. It can be seen that with no illumination the depletion region extends to the n^+ region. Reverse bias IV characteristics for different levels of illumination are shown in *fig. 7*. Internal potential and electric field distributions do not change significantly between dark and light conditions.

The current response of the device when illuminated with two different optical pulse shapes is shown in *fig. 8*. The first example is a perfectly square

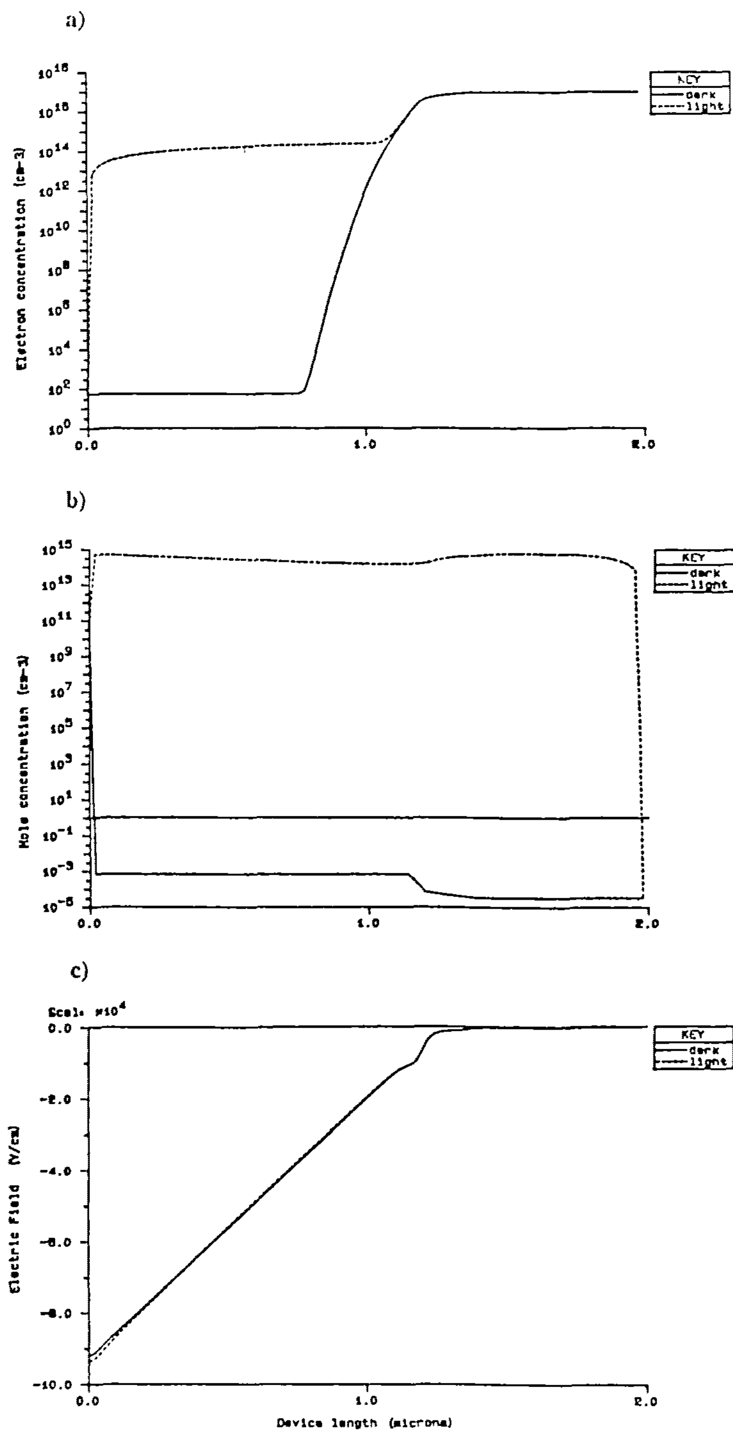

Fig. 6 Steady-state internal distibutions, (a) electron concentration, (b) hole concentration, (c) electric field

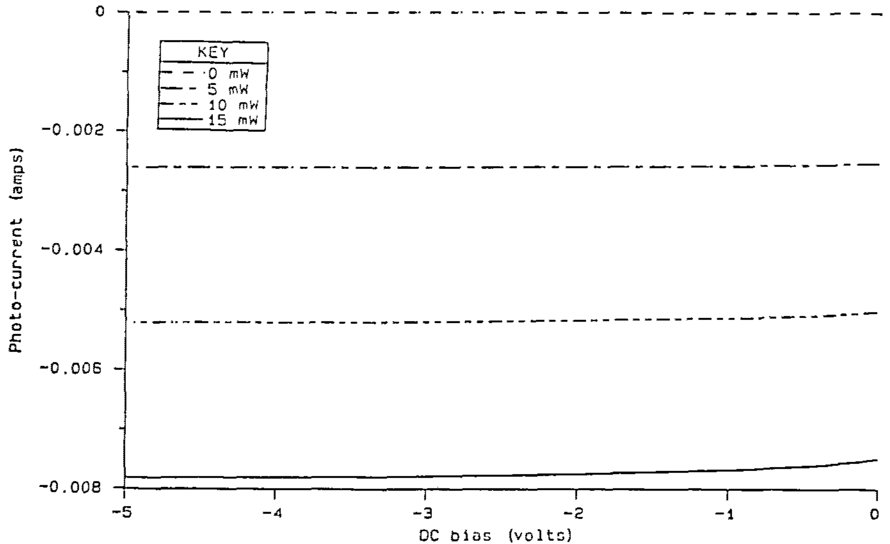

Fig. 7 Reverse bias IV characteristics

10 ps pulse with an incident power of 15 mW, this generates a detector response pulse with a FWHM of 10 ps. The second is a simple cosine with a FWHM of 10 ps and 15 mW peak incident power which generates a detector response with a FWHM of 15 ps. The difference between the two pulses is most significant in their rise times, the response to the square optical pulse being much sharper. When there is no further illumination both pulses have a similar decay. To compare these results with experimental data it is necessary to model the device parasitics using a relevant circuit model. An additional problem when making such measurements on these time scales is, when using the fastest sampling scope available, with 25 ps rise time, the results will still be scope limited.

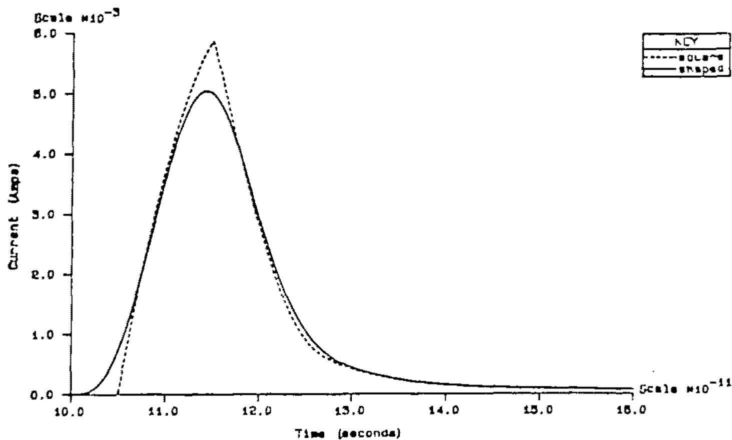

Fig. 8 Device response to 10ps pulses

Results from the Monte Carlo device simulation will be given during the presentation.

Conclusions

Monte Carlo and drift-diffusion models have been described for a high speed GaAs Schottky photodiode. An expression for the hole mobility as a function of electric field has been fitted to the results from the Monte Carlo simulation and used in the drift-diffusion model. Steady-state and transient results from the drift-diffusion model have been presented. These models have supplied a physical insight into the operation of such devices under the influence of ultra-short optical pulses.

Acknowledgements

This work is supported by the Science and Engineering Research Council and GEC Research Limited.

References

Barry, D. M., Snowden, C. M. and Howes, M. J. (1988). "A Numerical Simulation of High Speed GaAs Photodetectors", *IEE Colloquium on Microwave Devices, Fundamentals and Applications,* pp 5/1-5/6.

Brennan, K. and Hess, K. (1984). "Theory of high-field transport of holes in GaAs and InP", *Physical Review B* Vol. 29, pp 5581-5590

Costato, M., Jacoboni, C. and Reggiani, L. (1972). "Hole Transport in Polar Semiconductors", *Physica Status Solidi B,* Vol. 52, pp 461-473.

Holway, L. H., Steele, S. H. and Alderstein, M. G. (1979). "Measurement of Electron and Hole Properties in p-type GaAs", *Proceedings 7th Biennial Cornell Electrical Engineering Conference,* pp 199-208.

Jacoboni, C. and Reggiani, L. (1983). "The Monte Carlo method for the solution of charge transport in semiconductors with applications to covalent materials", *Reviews of Modern Physics,* Vol. 55, pp 645-705.

Littlejohn, M. A., Hauser, J. R. and Glisson, T. H. (1977). "Velocity-field characteristics of GaAs with $\Gamma_6^c - L_6^c - X_6^c$ conduction-band ordering", *Journal of Applied Physics,* Vol. 48, pp 4587-4590.

Moglestue, C. (1984). "Monte-Carlo particle model study of a microwave photodetector", *IEE Proceedings Part I,* Vol. 131, pp 103-106.

Moglestue, C. (1986). "A Self-Consistent Monte Carlo Particle Model to Analyze Semiconductor Microcomponents of any Geometry", *IEEE Transactions on Computer-Aided Design,* Vol. CAD-5, pp 326-345.

Nag, B. R. (1972). "Theory of Electrical Transport in Semiconductors", *Pergamon Press*

Parker, D.G. (1985). "Use of Transparent Indium Tin Oxide to form a highly efficient 20 GHz Schottky Barrier Photodiode", *Electronics Letters,* Vol. 21, No. 18.

Parker, D.G. and Say, P. (1986). "Indium Tin Oxide/GaAs Photodiodes for Millimetric-Wave Applications", *Electronics Letters,* Vol. 22, No. 23, pp 1266-1267.

Parker, D.G., Say, P.G. and Hansom, A.M. (1987). "110 GHz High Efficiency Photodiodes Fabricated from Indium Tin Oxide/GaAs", *Electronics Letters,* Vol. 23, No. 10.

Peterson, R.L. (1987). "Numerical Study of Currents and Fields in a Photoconductive Detector", *IEEE Journal of Quantum Electronics,* Vol. QE-23, No. 7, pp. 1185-1192.

Scharfetter, D.L. and Gummel, H.K. (1969). "Large-Signal Analysis of a Silicon Read Dipole Oscillator", *IEEE Trans. Electron Devices,* ED-16, pp. 64-77.

Snowden, C.M, Howes, M.J. and Morgan, D.V. (1983). "Large-Signal Modelling of GaAs MESFET Operation", *IEEE Trans. Electron Devices,* ED-30 pp. 1817-1824.

Snowden, C.M. (1986). "Introduction to Semiconductor Device Modelling", *World Scientific Publishing Co Pte Ltd.*

Sobol, H. (1987). "The Application of Microwave Techniques in Lightwave Systems", *Journal of Lightwave Technology,* LT-5, No. 3, pp.293-299.